

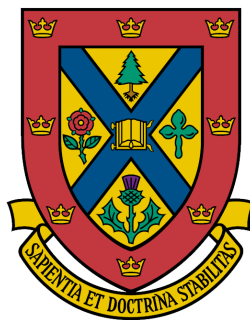
Design and evaluation of a repetitive-fire compact toroid fuelling system for ITER

by

GEOFFREY MICHAEL OLYNYK

Supervisor: Dr. Jordan Morelli, Ph.D., P.Eng.

A thesis submitted to the Department of Physics
in conformity with the requirements of the course
PHYS 455 – Engineering Physics Thesis



Queen's University
Kingston, Ontario, Canada
March, 2007

Abstract

A design is presented for a repetitive-fire compact toroid injection fuelling system for the ITER (2001) tokamak. Advantages of central over edge fuelling include plasma density control and higher deposition rates, implying lower tritium usage. The reference design offers $50 \text{ Pa m}^3 \text{ s}^{-1}$ of 90%D/10%T fuelling. 1.29 mg CTs are injected at a rate of 50 Hz (in order to synchronize with the European power grid) and a speed of 300 km s^{-1} . A new six-degree-of-freedom model of CT trajectory in the tokamak is developed and applied to the proposed injector design. The fueller is intended to work in parallel with the $500 \text{ Pa m}^3 \text{ s}^{-1}$ edge gas puffing system and to replace the centrifuge pellet-injection system in the ITER (2001) reference design. Each injected CT adds only 0.68% to the plasma inventory, implying that the injection process will be non-disruptive. Power consumption will be approximately 15 MWe. The strengths of the design compared to the current pellet injection system are highlighted.

Acknowledgements

I would like to thank my supervisor, Dr. Jordan Morelli, for his insight and support. Additionally, I would like to thank Dr. Morelli for giving me the chance to pursue this topic for my thesis; I consider myself very lucky to be able to research such a cutting-edge topic as part of my undergraduate career.

I also thank Dr. Chris Thurgood of the Royal Military College of Canada for training me in the use of Comsol Multiphysics, without which much of the important modelling in this project could not have been completed.

Contents

1	Introduction	1
1.1	Fusion Energy	1
1.2	Fuelling Requirements	2
2	Literature Review	4
2.1	Compact Toroids	4
2.2	The Conducting Sphere Model	4
2.3	Experimental Work	6
2.4	Application to ITER	7
3	Purpose	8
4	Main Design Considerations	9
4.1	Physical Size	9
4.2	Power Requirements	9
4.3	Neutral and metallic leakage into reactor	10
4.4	Repeatability	10
4.5	Reactor Stability	10
5	Choice of Physical Parameters	11
5.1	CT Size & Density	11
5.2	CT Initial Injection Angle	11
6	CT Dynamics Investigation	12
6.1	Development of Equations	12
6.2	Modelling Procedure	13
6.3	CT Trajectory Results	15

7	Design Overview	18
8	Other Design Considerations	20
8.1	Materials Selection	20
8.2	Gas Puffing Design	21
8.3	Power Supply	22
8.4	Fuel Handling	22
8.5	Shielding	23
8.6	Maintenance	23
9	Comparison to Alternative Systems	24
9.1	Edge Gas Fuelling	24
9.2	Pellet Fuelling	24
10	Discussion & Conclusions	26
10.1	Modelling Limitations	26
10.2	Theory Limitations	26
10.3	Conclusions	26
	References by Section	28
A	Glossary	38
A.1	Variables & Symbols, Roman	38
A.2	Variables & Symbols, Greek	38
A.3	Terminology	39
B	Supporting Calculations	40
B.1	Fuelling Rate	40
B.2	Euler-Lagrange Equations for CT Motion	40
C	Design Drawings	41

List of Tables

1	ITER (2001) operating parameters	14
2	Proposed CT injector parameters	18
3	Sequencing of events for each shot	21
4	Variables & Symbols, Roman	38
5	Variables & Symbols, Greek	38
6	Terminology	39

List of Figures

1	Overview of ITER (2001) tokamak	2
2	Edge gas puffing vs. central fuelling	3
3	Conducting sphere model of a CT	5
4	CT dynamics in 2D CS model	6
5	Cross-sectional view of ITER	9
6	CT dipole rotation angles	12
7	CT trajectory, X-Y	15
8	CT trajectory, R-Z	16
9	CT “dipole angle”	17
10	Overview of proposed gun design	18
11	ITER tokamak and injection ports	42
12	Detailed view of gun layout	43
13	Render of curved drift tubes	43

1 Introduction

1.1 Fusion Energy

Humanity has seen a progression of primary energy sources from those which have a high environmental impact – CO₂ emissions, clearcutting, smog – to modern sources which produce much less waste per joule. Today, we see widespread use of natural gas, which has the lowest carbon output of any fossil fuel, and nuclear fission power, which directly produces no CO₂ but has the disadvantage of producing long-lived radioactive isotopes as a waste product.

Nuclear fusion has the potential to continue this process and to be a widely used primary energy source. It has the potential to produce energy on the scale of nuclear fission or fossil fuels, with no greenhouse gas outputs and without producing any direct radioactive waste. Though it requires tritium as a fuel, which brings with it the possibility of environmental release, its half-life of 12.32 years is very short compared to the long-lived isotopes in the waste from nuclear fission plants.

The most promising reaction for controlled fusion is the deuterium-tritium (D-T) fusion reaction:



which offers the lowest Lawson criterion of any candidate reaction ($\sim 10^{21}$ keV s m⁻³). World-wide nuclear fusion research now centers around the development of a reactor called ITER, for which a schematic is shown in Figure 1. This device will function as the first test of a long-period (~ 1000 s) plasma burn with internal heating; that is, with the heat required to keep the plasma at its operating temperature supplied by the kinetic energy of the α particles emitted from the D-T reaction.

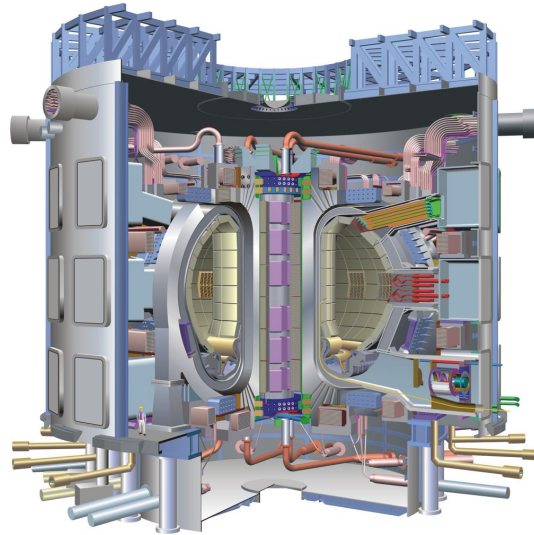


Figure 1: Cutaway view of ITER (2001) reference design showing reactor body, bioshield, and associated systems. (Courtesy International Atomic Energy Agency, Vienna, 2001.)

Construction has begun on ITER, with the first plasma discharges anticipated by 2016. While the design has been formalized in the document known as the ITER (2001) Technical Basis [1], changes are ongoing as the state of knowledge proceeds and new efficiencies and options are discovered [2].

1.2 Fuelling Requirements

In short plasma discharges, (< 1 s), enough gas can be injected into the reactor at the beginning to last through the entire discharge. This will not be the case in ITER, where steady-state operation for up to 1000 s is planned. Thus, fuelling during the discharge is required. There are two main options for accomplishing this: edge gas puffing, and central fuelling. A schematic of the two options is shown in Figure 2.

Edge gas puffing involves injecting the gas at the wall of the reactor and allowing it to diffuse into the plasma. As would be expected, this process has a very low efficiency and most of the fuel tends to circulate through the scrape-off layer (SOL), which is the layer of cool plasma between the hot core and the wall [3]. The alternative, central fuelling, involves injecting the deuterium/tritium fuel at a high velocity in order to have it penetrate to the

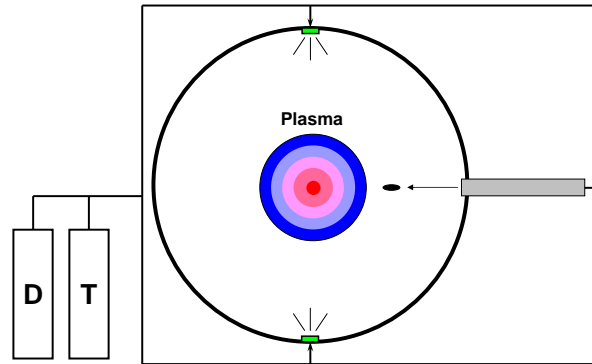


Figure 2: Schematic of edge gas puffing and central fuelling systems for tokamak fuelling. Central fuelling requires the injected fuel to have high velocity in order to penetrate to the plasma centre.

centre of the hot plasma. This paper offers a design for a central fuelling system for ITER based on injection of compact toroids.

2 Literature Review

2.1 Compact Toroids

Toroidal structures have long been recognized as a convenient way to isolate hot plasma from impurities and to maintain an equilibrium for longer than would otherwise be possible. Early experiments [1, 2] showed the possibility of creating rings with embedded poloidal fields (*i.e.* a toroidal z -pinch) and accelerating these rings down a coaxial drift tube using an apparatus known as a Marshall gun. The later development of the tokamak by Sakharov and Tamm [3, 4] ushered in the idea of rings with embedded poloidal *and* toroidal fields. This led to the development [5] of the compact toroid (CT), also known as the spheromak, which is a tokamak-like plasma configuration with no center “hole” and thus no toroidal field (TF) coils.

In 1982, Hartman & Hammer [6] proposed using a Marshall gun to accelerate spheromak-like plasma rings. The idea was proposed as a collective accelerator for “current drive, fueling, and heating of a conventional tokamak or other fusion reactor.” By the end of

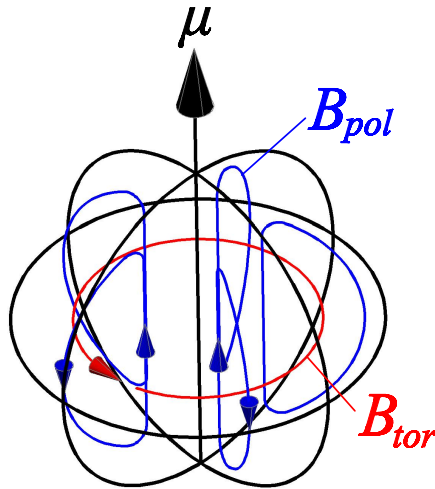


Figure 3: Conducting sphere (CS) model of a CT consists of a perfectly-conductive sphere (outlines shown in black) with embedded toroidal (red) and poloidal (blue) fields. Currents supporting these fields are opposite; I_{tor} is in the direction of B_{pol} , etc. Net magnetic dipole μ is shown as large black arrow.

the 1980s, the success of the “big tokamaks” – TFTR (USA, 1982), JET (UK, 1983) and JT-60 (Japan, 1985) – had led to the beginning of what was then called the International Thermonuclear Experimental Reactor (ITER). The initial phase of ITER development, known as the Conceptual Design Activities (CDA), began in 1988.

2.2 The Conducting Sphere Model

It was at this time that Parks [7] developed the Conducting Sphere (CS) model for the motion of a CT in a tokamak magnetic field. This model posits the CT as a perfectly conducting sphere with an embedded toroidal magnetic field (and thus a magnetic moment) which slips through the tokamak by displacing the field lines around it. Figure 3 shows a schematic of the fields embedded in the spherical CT. Perkins *et al.* [8] proposed using accelerated CTs as a fuelling method for reactor-grade plasmas in tokamaks by injecting them radially from the outboard side, and identified the required injection velocities, etc. that would be required for central penetration and reconnection. Figure 6 is a schematic of this injection and reconnection process for a CT injected into a uniform magnetic field.

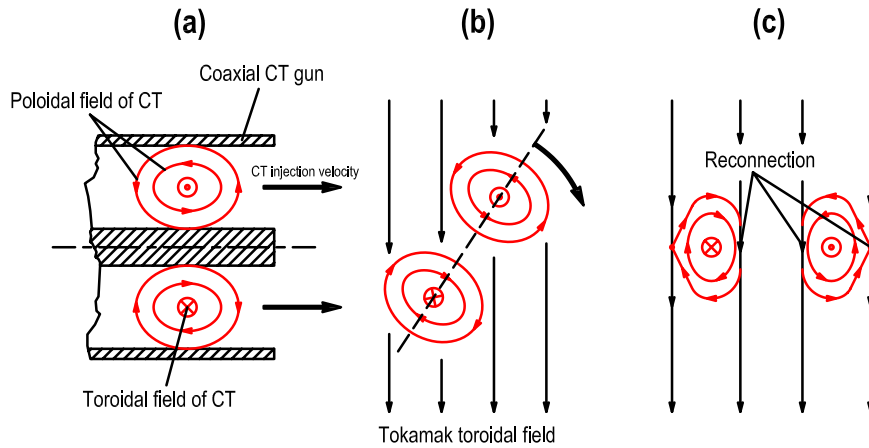


Figure 4: Process of (a) injection of CT, (b) tilting in tokamak toroidal field, and (c) reconnection at fuel deposition point (adapted from [8]). Vertical injection is as shown; for radial injection, magnetic field strength increases left-to-right.

Bozhokin [9] was the first to use the CS model developed by Parks in a Lagrangian form, non-dimensionalizing the equations and developing a functional form for the equations of motion in a cylindrical coordinate system. The CS model was developed further by Newcomb [10], who developed a more accurate model for the MHD wave drag. This is an effect by which the emission of Alfvén waves [11] slows the CT by a small amount as it travels. Xiao *et al.* [12] refined the work of Bozhokin and used the corrected (Newcomb) drag term, and also were the first to simulate [13] vertical (as opposed to radial) injection. It should be noted that all of these models had three degrees of freedom, considering the motion of the CT in a two-dimensional plane and the rotation of its dipole about a single fixed axis.

Hwang *et al.* [14] refined the CS model to include the effects of compressibility and non-zero tokamak beta (the ratio of plasma pressure to magnetic pressure). Suzuki *et al.* [15, 16] developed an alternative called the Non-Slipping (NS) model which included penetration into the CT of the tokamak magnetic field. Numerical simulation using the MHD equations showed the CT behaving in a manner in between the predictions of the CS and NS models.

2.3 Experimental Work

The theoretical development of models for CT motion in a tokamak was paced by experimental work in CT injection. Brown & Bellan [17] were the first to do so, injecting non-accelerated CTs with mass ~ 1 mg into Cal Tech's ENCORE tokamak. The particle inventory in the injected CTs, however, was 10 times that of the tokamak itself, and the injection process terminated the discharge. The first non-disruptive accelerated CT injection experiments were completed by 1994 using the Compact Toroid Fueller (CTF) device and the Tokamak de Varennes (TdeV) tokamak in Quebec [18]. CTs of mass between 10 and 60 μg were injected at speeds between 120 and 220 km s^{-1} . Work at TdeV continued with an investigation of the metallic impurities carried into the tokamak during the CT fuelling [19].

Further CT injection experiments were carried out at Cal Tech in the TEXT-U tokamak [20], in Japan's JFT-2M [21] and Large Helical Device [22], and more recently at UC Davis in the Compact Toroid Injection Experiment (CTIX) [23], this last experiment investigating only the CT acceleration process, without injecting into a tokamak. An investigation of the effect of the injection angle was completed using the University of Saskatchewan Compact Torus Injector (USCTI) firing ~ 1 μg CTs at 120 km s^{-1} into the STOR-M tokamak [13]. The U.S. Department of Defense has carried out the largest CT experiment ever conducted, entitled MARAUDER [24]. The device accelerated 2 mg CTs to a speed of 1000 km s^{-1} using a 9.36 MJ capacitor bank as a power supply.

Experiments on firing low-speed (~ 38 km s^{-1}) CTs horizontally and bending their trajectory 45° and 90° were first carried out at the Japanese Atomic Energy Research Institute (JAERI) in 2004 [25], with the conclusion that CTs will travel through such a bent drift tube "without any appreciable change in the CT parameters" [25]. Non-disruptive vertical CT injection into the top of the STOR-M tokamak was recently completed at U. Sask. at approximately 100 km s^{-1} through a 90° stainless-steel drift tube, from which it was concluded that CTs with a velocity up to 130 km s^{-1} "can be deflected successfully to the

vertical direction” [26]. This orientation has an advantage over outboard injection in that lower injection velocities are required because the radial field gradient does not have to be overcome by the initial kinetic energy.

2.4 Application to ITER

Many theoretical papers [7, 9, 12, 15, 16] have used ITER or ITER-like reactors as test cases for the CT trajectory models. In addition, there have been at least two [27, 28] serious proposals to use horizontal CT injection as a central fuelling method for ITER. The latter of these [28] concluded that a CT fueller based on the U.S. Navy’s MARAUDER device, firing 2.2 mg CTs at a rate of 20 Hz and a speed of 300 km s^{-1} at a power input of 8 MWe was feasible using current technology. This study investigated all aspects of the problem, including CT trajectory, mechanical configuration, magnetic and neutron shielding, impurity control, power supplies, fuel handling, and maintenance.

3 Purpose

The objective of this work is to design a repetitive-fire compact toroid injector which will replace the pellet-injection central fueller in the ITER (2001) reference design. This gun will be oriented in the standard (horizontal) position but will bend the CTs through a drift tube in order to take advantage of vertical injection.

The design will include specific details such as dimensions and construction materials for the formation, acceleration, and drift tube regions of the gun, injected CT magnetic field strength and speed, firing rate, and expected power consumption. Details of the power supply itself are beyond the scope of this work, however, note is made of the energy per CT shot and the options for supplying this amount of energy in a short time.

Comparison to alternative fuelling systems is made and the strengths of the proposed design are noted.

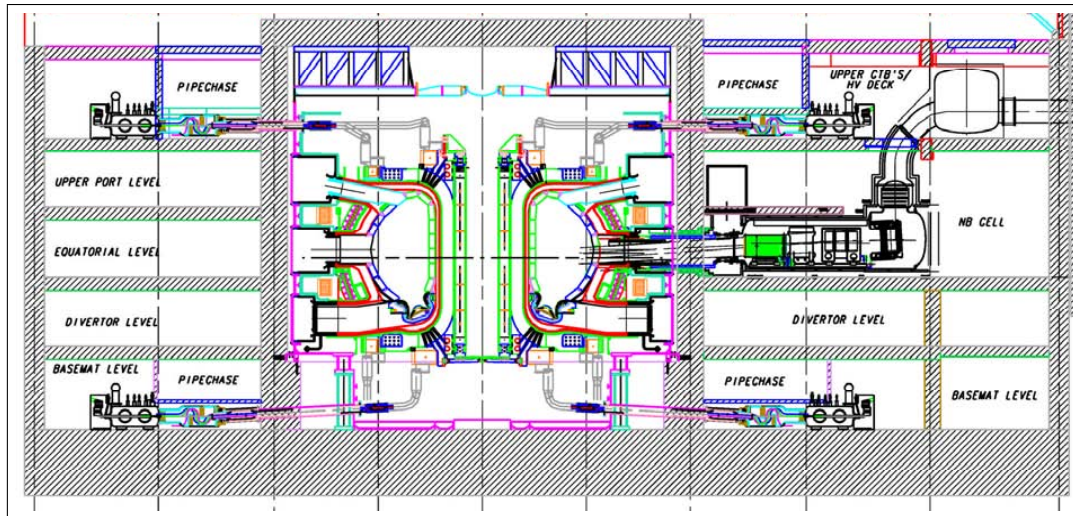


Figure 5: Cross-sectional view of ITER (2001) tokamak and support structures. From [1].

4 Main Design Considerations

4.1 Physical Size

The physical size of the gun is dictated by the CT radius, which is in turn a function of the CT density and mass. The drift tube and CT barrel must be able to be installed at the upper port level of the ITER complex [1] in order to achieve vertical injection. Figure 5 shows an overview of the ITER building (from [1]); the gun will be installed at the upper port level and drift tubes will be used to angle the CT to the selected injection angle.

4.2 Power Requirements

The power requirements can be naively calculated as the product of the energy per injected CT and the firing rate. However, this will give an under-estimate due to inefficiencies in the firing process. The actual power requirements are estimated using results from previously-built CT injectors, extrapolated to the size required for the ITER injector.

4.3 Neutral and metallic leakage into reactor

An ideal CT injector gun would send *only* fully ionized plasma rings out its barrel. In reality, two unwanted effects enter - cold neutral atoms, and metallic impurities. Neutral leakage is when the gas injected into the formation region is not ionized and entrained in the CT, and diffuses out the barrel and into the plasma in this “cold” state. This is unwanted because it saps energy from the plasma as it is heated up. This effect is minimized by proper design of the fast gas puffing valves. Coupling of injected gas to the ionized CT can be quite efficient: values as high as 50% [2] have been reported.

Metallic impurities are much more serious since they radiate bremsstrahlung at their (very numerous) x-ray emission frequencies. It has been calculated [3] that the tungsten ion density in the ITER (2001) reactor can be no more than $7 \times 10^{15} \text{ m}^{-3}$ for continued operation; even at this level, radiated losses equal half the input heating power. These impurities are entrained in the CT from the inner walls of the injector; materials must be chosen to minimize this effect.

4.4 Repeatability

The ITER reactor is expected to be in operation for approximately 20 years [4] in its main and extended phases of operation, and a single discharge can be as long as 1000 s. It is anticipated that there will be approximately 40,000 discharges during the ITER lifetime [5]. If the CT injector is firing 50 times per second during this time, 2×10^9 CTs will travel down the barrel. The requirements for wall refacing must be evaluated.

4.5 Reactor Stability

In past experiments [6], the CTs have been large and fast enough compared to the tokamak plasma itself that they destabilize the discharge and end it. It must be ensured that this will not occur in the ITER using the proposed fueller design.

5 Choice of Physical Parameters

5.1 CT Size & Density

A fuelling rate of $50 \text{ Pa m}^3 \text{ s}^{-1}$ implies a CT mass of 1.29 mg; the details are contained in Appendix B.1. A final injected CT radius of 0.1 m is chosen for three reasons. First, it is desired to have as little cross-sectional area protrude into the reactor as possible. Though the duct leading from the upper reactor hall is over 2 m in width [1], a pipe of this size leading into the reactor itself would be untenable. Second, it is known to be possible to compress CTs to this small size (20 cm diameter), as this was the final size of the CTs produced in the MARAUDER experiments [2]. Finally, the dynamics of the acceleration process mean that the CT is accelerated as it is compressed, making it much easier to accelerate to the design speed if the CT is compressed at the same time. The CT density (assuming its shape is approximately spherical) is then calculated to be $3.08 \times 10^{-4} \text{ kg m}^{-3}$. Each CT contains $N = 2.66 \times 10^{20}$ ions.

5.2 CT Initial Injection Angle

It is desired that the CTs have little residual vertical or radial velocity at reconnection, in order to not bend the tokamak field lines too severely. This is normally achieved by injecting the CT radially and attempting to have reconnection occur at the same time as the reversal of direction due to the field gradient [3]. This process, however, requires either very weak CT magnetic fields (difficult to achieve while obtaining high accelerations), or low CT densities (and thus large sizes) in order that the CT rotation not occur much faster than the linear motion. Vertical CT injection solves this problem by having the CT already at the vertical midplane of the tokamak, with the disadvantage that the lack of field gradient in the vertical direction means that the CT will have a large residual vertical velocity at reconnection. It is thus desirable to aim the gun ‘down the reactor’, that is, bent toroidally. The actual angles used are described in Section 6.

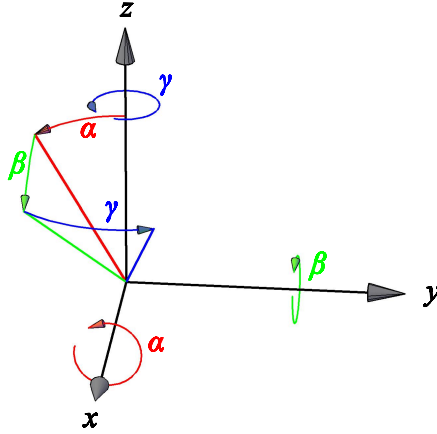


Figure 6: Rotation angles about degenerate body axes for CT dipole in extended CS model. Degenerate body axes (x, y, z) correspond to global tokamak axes (X, Y, Z) .

6 CT Dynamics Investigation

6.1 Development of Equations

To describe the motion of the CT inside the tokamak, the three-degree-of-freedom conducting sphere (CS) model developed by Bozhokin [1], Newcomb [2], and Xiao et al. [3] was extended to a full six degrees of freedom. The motion of the CT is then described by the Lagrangian:

$$\begin{aligned}
 \mathcal{L} = & \underbrace{\frac{1}{2} m_{CT} (\dot{R}^2 + R^2 \dot{\phi}^2 + \dot{Z}^2)}_{\text{linear kinetic}} + \underbrace{\frac{1}{5} m_{CT} r_{CT}^2 (\dot{\alpha}^2 + \dot{\beta}^2 + \dot{\gamma}^2)}_{\text{rotational kinetic}} \\
 & - \underbrace{\frac{B_0^2 R_0^2}{2\mu_0 R^2} \frac{4}{3} \pi r_{CT}^3}_{\text{magnetic field exclusion}} - \underbrace{\frac{k B_{CT}}{\mu_0} \frac{4}{3} \pi r_{CT}^3 \frac{B_0 R_0}{R}}_{\text{dipole / tokamak interaction}} \times \\
 & \underbrace{(\cos \alpha \sin \beta \cos \gamma \sin \phi + \sin \alpha \sin \gamma \sin \phi + \sin \alpha \cos \gamma \cos \phi - \cos \alpha \sin \beta \sin \gamma \cos \phi)}_{\text{dipole / tokamak field interaction (cont'd)}} \quad (2)
 \end{aligned}$$

where cylindrical coordinates $(R, \phi, Z) = \left(\sqrt{X^2 + Y^2}, \tan^{-1} \left(\frac{Y}{X} \right), Z \right)$ from an origin at the

center of the tokamak are used. The rotation angles (α, β, γ) are about the degenerate body axes as shown in Figure 6. The other symbols in (2) are as follows: m_{CT} is the mass of the CT [kg], r_{CT} is the CT radius [m], R_0 is the tokamak major radius [m], B_0 is the toroidal magnetic field at $R = R_0$ [T], and B_0 is the embedded CT toroidal magnetic field [T]. The coupling constant k , which controls the interaction strength between the CT dipole and the tokamak field, was set at 1 in the final simulation. The drag force due to MHD wave emission [2] can be described by the following Rayleigh dissipation term:

$$\mathcal{F} = \pi \rho r_{CT}^2 I V_A \times \left(\dot{R}^2 + R^2 \dot{\phi}^2 + \dot{Z}^2 \right) \quad (3)$$

where ρ is the plasma density in the tokamak [kg m^{-3}], $V_A = \frac{B_0}{\sqrt{\mu_0 n_0 m}}$ is the Alfvén speed [m s^{-1}] and I is a dimensionless coefficient derived by Newcomb [2]:

$$I = \frac{V_s}{V_A} \left[\frac{2}{9} \left(1 + \ln \frac{V_A}{V_s} \right) - 0.37 \right] \quad (4)$$

where the term V_s in (4) is the sound speed $V_s = \sqrt{\gamma Z k_B \frac{T_e}{m_i}}$ [m s^{-1}] in which γ is the adiabatic index, and T_e and m_i are the electron temperature [K] and ion mass [kg], respectively. The Euler-Lagrange equations (6 in total) are then:

$$\frac{d}{dt} \left(\frac{\partial \mathcal{L}}{\partial \dot{q}_j} \right) - \frac{\partial \mathcal{L}}{\partial q_j} + \frac{\partial \mathcal{F}}{\partial \dot{q}_j} = 0 \quad (5)$$

The actual form of these equations is worked out in Appendix B.2.

6.2 Modelling Procedure

The operating parameters for ITER (2001) in Hybrid #1 operation mode (see [4]) were used for simulation of the CT motion; they are summarized in Table 1. Hybrid #1 is one

Table 1: ITER (2001) operating parameters (from [4]).

Major radius, R_0 [m]	6.2
Minor radius, a [m]	2.0
Toroidal magnetic field, B_0 [T]	5.3
Plasma density, $n_e = n_i = n_0$ [m^{-3}]	9.3×10^{19}
Averaged ion temperature, $\langle T_i \rangle$ [keV]	8.4
Averaged electron temperature, $\langle T_e \rangle$ [keV]	9.6

of three operating modes proposed for ITER; it is envisioned as a “half-way point” between the basic inductive operating mode and true steady-state (non-inductive) operation [4]. It is used here as a proof of concept; the model is readily adaptable to the other modes by simply adjusting the parameters (plasma density, magnetic field, etc.). The CT was chosen to have a radius of 0.1 m and a mass of 1.29 mg, as described in Section 5. The CT magnetic field strength was chosen to be 0.4 T in the model. This is the level at which CT toroidal magnetic fields were measured in the CTIX experiment [5].

The equations were solved using COMSOL Multiphysics 3.3 using a finite-difference minimization method over 2000 mesh points spanning dimensionless times $0 < \tau < 18$, where $\tau = \frac{V_A}{R_0} t$. The convergence criteria was set so that residuals were less than 1 part in 10^6 . The dipole/tokamak field coupling parameter k was initially set to 0 and then ramped up in steps of 0.1 to its final value of 1, in order to improve convergence. Each solution took approximately 30 s to converge on a 2.4 GHz processor.

This solution procedure was repeated manually several times, varying the injection angle of the CT, as well as the initial velocity $V(\tau = 0)$ until a solution was reached for which the following criteria were met:

- The CT passed through (or near) the center of the tokamak, that is, $R \approx R_0$ when $Z = 0$.
- The angle between the CT dipole and the tokamak magnetic field was less than 0.5° . This was a somewhat arbitrary choice, but should be sufficient to ensure reconnection of the CT poloidal magnetic field with the tokamak toroidal field [6, 7].

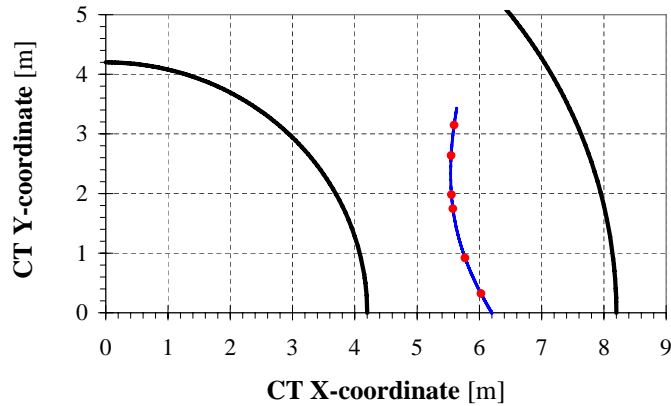


Figure 7: Calculated trajectory of CT, looking down from top of tokamak. Thick black lines are the tokamak walls at midplane ($Z = 0$), blue is CT trajectory. Red circles indicate possible deposition points, with most likely deposition at the last point shown, at $t = 13.6 \mu\text{s}$.

6.3 CT Trajectory Results

The initial velocity and gun angle were obtained using the manual optimization procedure described in Section 6.2, with the result that an injection velocity $V_0 = 300 \text{ km s}^{-1}$ should be used. The gun should be mounted at a poloidal angle of 90° (that is, at the top of the tokamak). The injection point is then rotated at an orientation of 60° toroidally, so that the CT is injected along the toroidal axis of the tokamak. In addition, the gun is rotated 30° inwards (about the global Z axis) so that the CT has some initial velocity in the (negative) radial direction.

The calculated CT path is shown in Figures 7 and 8. The red circles are those points for which the “dipole angle” (that is, the angle between the CT dipole and the tokamak magnetic field) reaches a minimum. CT reconnection and fuel deposition could conceivably occur at any of these points. Given the lack of empirical results or theoretical modelling as to the actual dipole angle required for reconnection, the criterion was selected that the dipole angle must be less than 0.5 degrees. This implies that the reconnection will occur at the last point (at $t = 13.6 \mu\text{s}$).

At reconnection, the CT has a residual velocity of 288 km s^{-1} (151 km s^{-1} toroidally, 201 km s^{-1} toroidally, and -139 km s^{-1} vertically). This will have two main effects:

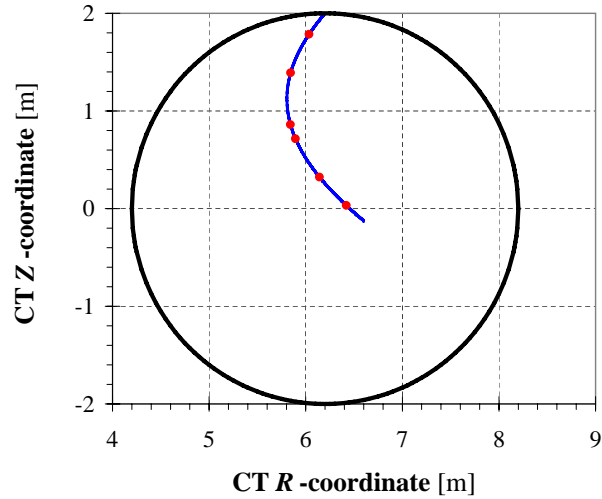


Figure 8: Calculated trajectory of CT in R-Z plane, moving through ϕ with CT. All paths/points as in X-Y trajectory plot.

- a Due to the non-zero reconnection time, the fuel will be “smeared” over a certain range, rather than being deposited right at the center. While many early models [6, 8, 1] assume that reconnection is instant at field alignment, it has been estimated [9, 10] (using the Sweet-Parker current sheet model) that the time scale for CT reconnection is $\tau_{rec} = \sqrt{\tau_A \tau_R}$, where τ_A is the Alfvén time scale and τ_R is the resistive diffusion time scale. For the CTs examined here, this corresponds to about $3 \mu s$, during which time the CT will travel about 90 cm. This is almost $\frac{1}{2}$ of the minor radius of the ITER reactor.
- b The residual CT momentum of 0.37 kg m s^{-1} will be transferred to the plasma. However, most of this momentum is in the toroidal direction where it will simply contribute to the toroidal current and not cause the plasma to hit the walls.

The dipole angle is plotted as a function of time in Figure 9. As discussed above, it can be seen that there are several points at which the CT may undergo reconnection; the model developed here is not advanced enough to predict whether this will actually occur.

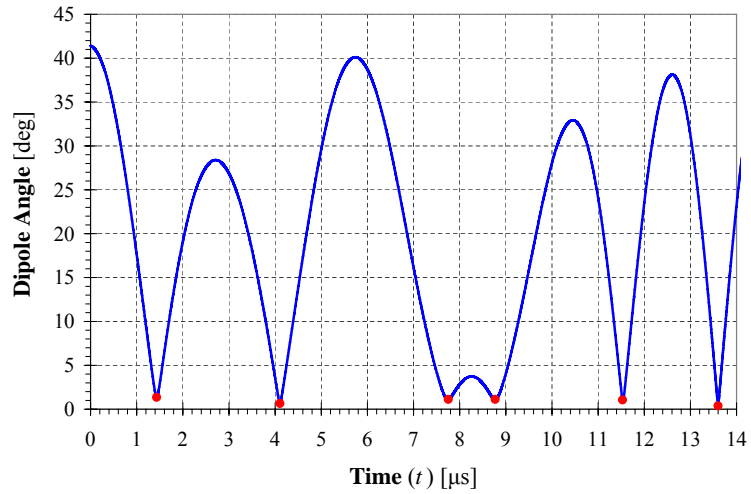


Figure 9: Calculated angle between CT dipole and tokamak magnetic field as a function of time. Red dots indicate minima; only the sixth such minimum (at $t = 13.6 \mu\text{s}$) meets the 0.5° criterion.

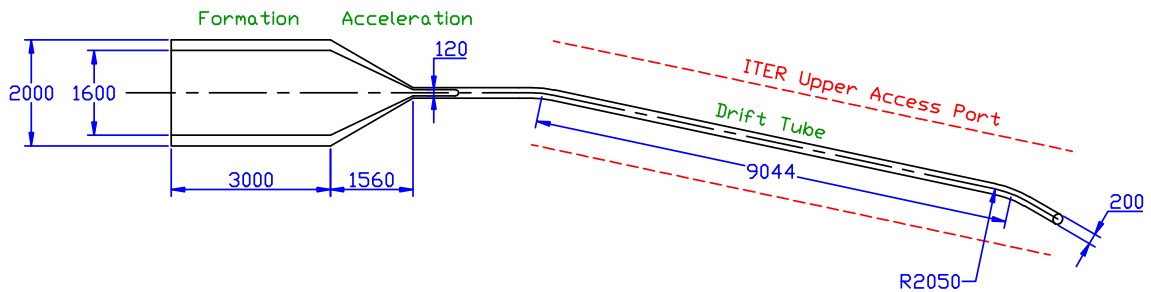


Figure 10: Overview of proposed gun design showing formation and acceleration regions, as well as long drift tube of inner diameter 0.2 m. All drift tube radii of curvature are 2.05 m.

7 Design Overview

A technical drawing of the proposed gun design is shown in Figure 10. More detailed drawings of each part are shown in Appendix C. Finally, a summary of the important gun parameters is shown in Table 2.

The radius of curvature for the two bends in the drift tube was chosen to be 2.05 m, based on extrapolation from current work in drift tubes [1]. In the STOR-M vertical injection experiments, a CT was successfully bent (without noticeable effect) through a drift tube of radius 0.164 m at a speed of 120 km s^{-1} . Here, the CT is twice the diameter (20 cm vs. 10 cm.) and the speed is 2.5 times higher. The required radius of curvature scales directly

Table 2: Summary of important parameters (dimensions, etc.) for proposed CT injector.

Parameter	Description
Radius, formation region	1 m
Radius, end of gun barrel	0.1 m
Radius of curvature	2.05 m
Shot voltage	3.5 kV

with the CT diameter and would be expected to scale with the centrifugal force (thus the speed squared). A radius of 2.05 m was thus chosen.

The annular formation region has an inner radius of 0.8 m and an outer radius of 1.0 m, giving 20 cm for formation. This distance has been chosen to be comparable with past designs [2, 3, 4]. The 3.5 kV formation and acceleration voltages are also chosen based on past experiments; no modelling of the firing process has been done in this paper. It is noted that there is 0.86 m of cantilevered inner electrode with a diameter of 0.12 m in the later part of the acceleration region. This is of a comparable ratio to past designs [4] and thus it is not anticipated that it will be a problem. If, however, a tungsten-coated copper electrode has too much “sag” in it, the option remains to bolster the center core with a reinforcing material such as steel or titanium, as this area will never be exposed to the plasma.

8 Other Design Considerations

8.1 Materials Selection

Past CT injectors and drift tubes [1, 2, 3, 4] have usually been built using stainless steel as a plasma facing material. However, these guns have always been used for short bursts (either single shots, or ~ 100 at a time [5]). The proposed ITER fueller, in contrast, will require up to 50,000 injections *per discharge*, and must operate for long periods of time (thus numerous discharges) between maintenance intervals.

Tungsten, with the highest energy threshold for sputtering due to plasma contact [6, 7] is thus a natural choice for the CT injector body to be constructed from. A tungsten coating is being developed for some regions of the divertor [8], where the plasma impinging on the wall is of a much higher energy and irradiance. Proper conduction of the formation and acceleration charges through the gun requires a copper backing, and thus a tungsten / copper bonding process [7] will be used.

It is experimentally known that CTs are very poor at entraining tungsten from the walls of the gun and drift tube as they travel. One estimate of the upper limit of tungsten contamination in the CT is 2×10^{-5} W atoms per CT atom [9]. Assuming that this worst-case scenario is realized in the ITER injector, each CT will carry 5.33×10^{15} W ions into the reactor, or 2.66×10^{17} W ions per second. The steady-state W concentration in the reactor then depends on the mechanism by which it diffuses out and depends on poorly-understood phenomena such as impurity transport barriers [10]. However, it is noted that even in this worst-case scenario, over a 1000 s discharge 2.66×10^{18} W ions will be carried into the reactor, a ratio of 5.8×10^{-5} to the total ion number in the tokamak. The allowable tungsten density is 0.01% (or 10^{-4}) of electron (and ion) density. Thus, even in the worst-case tungsten entrainment scenario, with *no* W diffusion out of the reactor, it should not be a problem for reactor operation.

8.2 Gas Puffing Design

Fast piezoelectric gas puffing valves are required to be placed azimuthally around the inner wall of the formation region (see Figure 10). It is desired that as little gas as possible leak down the barrel of the gun and into the reactor without being ionized and formed into a CT. It is known from past experiment [5] that coupling of $\geq 50\%$ can be achieved.

While it is possible to calculate the gas passing through a piezoelectric valve using a one-dimensional collisionless flow approximation [11], it is more accurate to use an experimental correlation developed as part of the MARAUDER project [5]:

$$m(t) = \left(0.128 \frac{\text{mg}}{\mu\text{s}}\right) (35.71\mu\text{s}) \left[1 + \exp\left(\frac{t - 636.3\mu\text{s}}{35.71\mu\text{s}}\right)\right] \quad (6)$$

which gives the gas passing through 60 piezoelectric gas puffing valves at a plenum pressure of 100 psig. The MARAUDER design has a formation-region radius of 0.5 m, half that of the proposed ITER fueller. It is thus desirable that four times the number of gas valves (240) be used in order to maintain good azimuthal distribution of gas upon injection. Given this number of valves, gas must pass through for 677 μs per shot in order to allow 2.6 mg of gas to enter into the ionization region. Table 3 then outlines the sequence of events that occur every $\frac{1}{50}$ s.

Table 3: Sequence of events that occur in each firing of the CT injector gun.

Time	Event
677 μs	Gas injection
$\sim 5 \mu\text{s}$	Ionization pulse
15 μs	Wait
$\sim 10 \mu\text{s}$	Acceleration pulse
33 μs	CT travels down drift tube
19.26 ms	Acceleration pulse

8.3 Power Supply

The MARAUDER gun [5], of similar size to the proposed ITER fueller, was estimated to have up to 30% acceleration efficiency [12], neglecting formation energies. Experimental results indicated that 1 mg CTs injected at 400 km s⁻¹ (80 kJ CT kinetic energy) required up to 400 kJ of capacitor-bank energy, an efficiency of 20%. This lower efficiency is used here; it should be regarded as a worst-case scenario which may be improved upon with further developments.

The 1.29 mg CTs injected at 300 km s⁻¹ each have a kinetic energy of 58.1 kJ. At a firing rate of 50 Hz and an efficiency of 20%. This implies a power consumption of 14.5 MW, which is about 2% of the total fusion power output of 700 MW in Hybrid #1 operation

mode [13], a very large power draw. It should be noted that this neglects residual power requirements such as operating the gas puffing valves and any diagnostic systems. However, these systems will draw power on the order of hundreds of watts only and are thus negligible compared to the main power required for the injector.

8.4 Fuel Handling

The fuel supply for the injector will be the same as that of the pellet-injection system. The 90%T/10%D fuel mixture is piped from the fuel cleanup/supply systems (located in the tritium plant, in a separate building) through one of the “ring manifolds” which are located in the reactor building itself [14]. One 7 mm fuel line will carry T₂ and one 16.5 mm fuel line will carry a DT mixture [13], which together supply the entire fuelling system (including the 400 Pa m³ s⁻¹ required for the edge gas puffers). It should be noted that tritium containment for the proposed CT injector is considerably simpler than for the pellet injection system, since freezing / pellet formation using a screw ejector [13] is not required.

All components of the gun contain vacuum and are thus (a) at a negative pressure relative to the rest of the building and (b) built to high-vacuum standards, implying a very low leakage rate. In the event of a tritium / DT leak from the injector fuelling systems, the already-developed leak detection strategies [13] will be sufficient to identify and repair the leak. In the case of a large leak, the reactor building is equipped with an isolated ventilation system which can prevent T₂ release to the environment.

8.5 Shielding

The sensitive equipment in the formation region will not be directly exposed to the 14 MeV neutron flux from the reactor, due to the structure of the gun. The neutron flux will impact the conical acceleration region where it will be activated to a higher degree than stainless

steel would be [7] and thus presents a higher liability for safe storage and disposal during the months [7] when most of the high-level isotopes will decay.

Assuming the rate of tungsten loss is the worst case scenario (5.33×10^{15} W atoms per CT), the cladding over the entire plasma-facing surface area of $\sim 50 \text{ m}^2$ will lose approximately 1.7×10^{-15} m per CT, or less than 1 nm per 1000 s ITER discharge. The shielding life will be dictated by neutron activation, not material loss due to sputtering.

8.6 Maintenance

The main body of the gun will be in the upper port room outside the bioshield and cryostat, which significantly eases maintenance requirements. (Note, however, that it means that leak-tightness must be validated to a tighter standard than it would be within the bioshield for reasons of environmental contamination.)

Relining of the gun barrel with tungsten will require removal from the reactor body and thus a loss of vacuum. Maintenance of the CT injector will therefore be conducted during scheduled reactor maintenance periods.

9 Comparison to Alternative Systems

9.1 Edge Gas Fuelling

Though the proposed CT injector is intended to complement, not replace, the edge gas puffing system, the differences between the two are worth discussing here. The edge gas fuelling system is larger ($400 \text{ Pa m}^3 \text{ s}^{-1}$ for edge vs. $50 \text{ Pa m}^3 \text{ s}^{-1}$ for the proposed CT central fuelling system). These numbers are not directly comparable because transport of fuel to the hot core of the tokamak is limited by diffusion for edge gas fuelling. Most of the

edge-injected fuel simply circulates in the scrape-off layer, a sheath of cold plasma between the hot core and the wall, and then exits through the divertor venting system [1].

In contrast, fuel injected to the center is more efficiently coupled to the fusion reactions [1], and is necessary to maintain a flat density profile throughout the plasma column. (Diffusion from the edge would require the fuel density to be lower in the core of the plasma.)

9.2 Pellet Fuelling

The proposed CT injector fuelling system is intended to replace the pellet fuelling system. There are three main advantages. The first is mechanical simplicity. While the CT fueller requires a high-voltage power supply and fast gas puffing valves, a pellet fueller requires a freezing system to make deuterium/tritium ice, a pellet-creation system (currently envisioned as a screw injector [2]) and a high-velocity centrifuge or pneumatic gun. Mechanical strength of the D/T “ice” pellets limits the maximal achievable velocity to approximately 1 km s^{-1} , a speed at which it takes 1 ms for the pellet to reach the core of the plasma. This is a comparatively long time and most of the pellet ablates away during the travel process, depositing the fuel throughout the reactor rather than in the core. In contrast, the CT reaches the core of the plasma very quickly and the localization of the fuel deposition is limited only by the reconnection time, in general a much faster process than pellet ablation. Thus the CT fueller has the capability for much better fuel localization than the pellet injection system, an important requirement for an experimental reactor in which a wide variety of tests are to be run.

It has been proposed [3] to use RF heating to inject a pellet at $\sim 3 \text{ km s}^{-1}$ by backing the deuterium/tritium “ice” pellet with a D_2 layer with embedded lithium particles. This “pusher” would then be heated by a high-intensity radiofrequency pulse and would vaporize and accelerate the pellet. While this method has the capability of higher velocities than the standard pellet injection system, it is still limited compared to the CT fueller in speed and

mechanical simplicity. This system would require both mechanical systems (pellet formers, etc.) *and* high-voltage equipment (gyrotrons and waveguides).

10 Discussion & Conclusions

10.1 Modelling Limitations

The numerical model of CT motion developed in Section 6 is only an approximation to the real structure of CTs, in several ways. First, CTs are not actually spheres; they are prolate ellipsoids, sometimes extremely so (up to 10 times longer than wide [1]). The CT is approximated as a perfectly conductive sphere, so that the tokamak magnetic field cannot penetrate it at all; this is also an approximation, though a better one. The magnetic field actually penetrates the CT, causing reconnection and disintegration over a time scale of approximately $40 \mu\text{s}$ [2], which is longer than the $\sim 16 \mu\text{s}$ required for the CT to travel to the center of the tokamak in the proposed fueller design.

10.2 Theory Limitations

There are several aspects of the proposed design which are extrapolated from past experimental devices. This includes the ability of the CT to travel through a curved drift tube, the entrainment of tungsten from the gun walls into the CT, the efficiency of acceleration, and the ability of the gun to compress the CT from a 1 m formation radius to a 0.1 m final radius. A more detailed feasibility study would have to be conducted before building the device in order to more closely predict the injector behaviour. The MARAUDER study [2] is an example of such a detailed study, including numerical MHD simulations of CT behaviour during the formation and acceleration phases.

10.3 Conclusions

A design has been presented for a central fueller for ITER based on repetitively fired compact toroids of mass 1.29 mg. With its design based on past experiments and new extensions to previously-developed theories, this fueller should deliver $50 \text{ Pa m}^3 \text{ s}^{-1}$ of 90%T/10%D fuel to a region approximately 1 m across in the center of the tokamak. The fueller, even with pessimistic assumptions for impurity entrainment, will not introduce an excessive amount of high-Z impurities to the plasma. Power consumption should be approximately 14.5 MWe, which is a significant fraction of the 40 MW of heating power for the reactor [3]. Nevertheless, the flexibility and control characteristics of the CT fueller make it an attractive choice compared to the status quo pellet injection fuelling system.

References: Section 1

- [1] International Atomic Energy Agency, “ITER Technical Basis,” International Atomic Energy Agency, Tech. Rep., July 2001, no. 19 in the ITER EDA Documentation Series.
- [2] C. Braams and P. Stott, *Nuclear Fusion: Half a Century of Magnetic Confinement Fusion Research*, 1st ed. Philadelphia: IOP Publishing Ltd., 2002.
- [3] R. Raman and P. Gierszewski, “Compact toroid fuelling for ITER,” *Fus. Eng. Des.*, vol. 39–40, pp. 997–985, 1998.

References: Section 2

- [1] H. Alfvén, L. Lindberg, and P. Mitlid, “Experiments with plasma rings,” *J. Nucl. Energy C*, vol. 1, pp. 116–120, 1960.
- [2] J. W. Mather, “Investigation of the high-energy acceleration mode in the coaxial gun,” *Phys. Fluids*, vol. 7, no. 11, pp. S28–S34, 1964.
- [3] A. Sakharov, “*Teoriya magnitnogo termoyadernogo reaktora* (the theory of magnetic fusion reactors), Pt. II,” in *Fizika Plazmy i Problema Upravlyaemykh Termoyadernykh Reaktsii (Plasma Physics and Problems of Controlled Thermonuclear Reactions)*, Vol. 1, M. Leontovich, Ed. Moscow: Izd. AN SSSR, 1958, p. 20.
- [4] I. Tamm, “*Teoriya magnitnogo termoyadernogo reaktora* (the theory of magnetic fusion reactors), Pt. II,” in *Fizika Plazmy i Problema Upravlyaemykh Termoyadernykh Reaktsii (Plasma Physics and Problems of Controlled Thermonuclear Reactions)*, Vol. 1, M. Leontovich, Ed. Moscow: Izd. AN SSSR, 1958, pp. 3, 31.
- [5] M. Bussac, H. Furth, M. Okabayashi, M. Rosenbluth, and A. Todd, *Plasma Physics and Controlled Nuclear Fusion Research*. Vienna: International Atomic Energy Agency, 1979, vol. 3, p. 251.

- [6] C. W. Hartman and J. H. Hammer, “New type of collective accelerator,” *Phys. Rev. Lett.*, vol. 48, no. 14, pp. 929–932, 1982.
- [7] P. Parks, “Refueling tokamaks by injection of compact toroids,” *Phys. Rev. Lett.*, vol. 61, no. 12, pp. 1364–1367, 1988.
- [8] L. Perkins, S. Ho, and J. Hammer, “Deep penetration fuelling of reactor-grade tokamak plasmas with accelerated compact toroids,” *Nucl. Fus.*, vol. 28, no. 8, pp. 1365–1378, 1988.
- [9] S. Bozhokin, “Motion of a compact torus in a tokamak plasma,” *Sov. J. Plasma Phys.*, vol. 16, no. 10, pp. 702–705, 1990.
- [10] W. A. Newcomb, “Magnetohydrodynamic wave drag,” *Phys. Fluids B*, vol. 3, no. 8, pp. 1818–1829, 1991.
- [11] H. Alfvén, “Existence of Electromagnetic-Hydrodynamic Waves,” *Nature*, vol. 150, no. 3805, pp. 405–406, 1942.
- [12] C. Xiao, A. Hirose, and W. Zawalski, “Trajectory of a compact toroid tangentially injected into a tokamak,” *Nucl. Fus.*, vol. 38, no. 2, pp. 249–256, 1998.
- [13] C. Xiao, O. Mitarai, A. Hirose, W. Zawalski, D. White, E. Furkal, D. McColl, R. Raman, R. Décoste, B. Gregory, and F. Martin, “Tangential CT injection and 1.5 cycle AC operation experiments on STOR-M,” in *Proceedings of the 16th IAEA Fusion Energy Conference*. International Atomic Energy Agency, 1997, pp. 595–601.
- [14] D. Hwang, M. Ryutova, and H. McLean, “Penetration of a compressible magnetized plasma object into a low beta target plasma,” *Phys. Plasmas*, vol. 6, no. 5, pp. 1515–1521, 1999.
- [15] Y. Suzuki, T. Hayashi, and Y. Kishimoto, “Theory and MHD simulation of fuelling by compact toroid injection,” *Nucl. Fus.*, vol. 41, no. 7, pp. 873–881, 2001.
- [16] —, “Effect of magnetic reconnection on CT penetration into magnetized plasmas,” *Earth Planets Space*, vol. 53, pp. 547–551, 2001.

- [17] M. Brown and P. Bellan, “Efficiency and scaling of current drive and refuelling by spheromak injection into a tokamak,” *Nucl. Fus.*, vol. 32, no. 7, pp. 1125–1137, 1992.
- [18] R. Raman, F. Martin, B. Quirion, M. St-Onge, J.-L. Lachambre, D. Michaud, B. Sawatzky, J. Thomas, A. Hirose, D. Hwang, N. Richard, C. Côté, G. Abel, D. Pinsonneault, J.-L. Gauvreau, B. Stansfield, R. Décoste, A. Côté, W. Zuzak, and C. Boucher, “Experimental Demonstration of Nondisruptive, Central Fueling of a Tokamak by Compact Toroid Injection,” *Phys. Rev. Lett.*, vol. 73, no. 23, pp. 3101–3104, 1994.
- [19] R. Raman, F. Martin, E. Haddad, M. St-Onge, G. Abel, C. Côté, N. Richard, N. Blanchard, H. Hai, B. Quirion, J.-L. LaChambre, J.-L. Gauvreau, G. Pacher, R. Décoste, P. Gierszewski, D. Hwang, A. Hirose, S. Savoie, B.-J. LeBlanc, H. McLean, C. Xiao, B. Stansfield, A. Côté, D. Michaud, and M. Chartré, “Experimental demonstration of tokamak fuelling by compact toroid injection,” *Nucl. Fus.*, vol. 37, no. 6, pp. 967–972, 1997.
- [20] J. Yee and P. Bellan, “Effects of CT injector acceleration electrode configuration on tokamak penetration,” *Nucl. Fus.*, vol. 38, no. 5, pp. 711–721, 1998.
- [21] T. Ogawa, N. Fukumoto, M. Nagata, H. Ogawa, M. Maeno, K. Hasegawa, T. Shibata, T. Uyama, J. Miyazawa, S. Kasai, H. Kawashima, Y. Miura, S. Sengoku, and H. Kimura, “Compact toroid injection experiment in JFT-2M,” *Nucl. Fus.*, vol. 39, no. 11Y, pp. 1911–1915, 1999.
- [22] J. Miyazawa, H. Yamada, K. Yasui, S. Kato, N. Fukumoto, M. Nagata, and T. Uyama, “Design of spheromak injector using conical accelerator for Large Helical Device,” *Fus. Eng. Des.*, vol. 54, pp. 1–12, 2001.
- [23] K. Baker, D. Hwang, R. Evans, R. Horton, H. McLean, S. Terry, S. Howard, and C. DiCaprio, “Compact toroid dynamics in the Compact Toroid Injection Experiment,” *Nucl. Fus.*, vol. 42, pp. 94–99, 2002.

- [24] J. Degnan, R. J. Peterkin, G. Baca, J. Beason, D. Bell, M. Dearborn, D. Dietz, M. Douglas, S. Englert, T. Englert, K. Hackett, J. Holmes, T. Hussey, G. Kiuttu, F. Lehr, M. G.J., B. Mullins, D. Price, N. Roderick, E. Ruden, C. Sovinec, P. Turchi, G. Bird, S. Coffey, S. Seiler, Y. Chen, D. Gale, J. Graham, M. Scott, and W. Sommars, “Compact toroid formation, compression, and acceleration,” *Phys. Fluids B*, vol. 5, no. 8, pp. 2938–2958, 1993.
- [25] N. Fukumoto, Y. Inoo, M. Nomura, M. Nagata, T. Uyama, H. Ogawa, H. Kimura, U. Uehara, T. Shibata, Y. Kashiwa, S. Suzuki, S. Kasai, and JFT-2M Group, “An experimental investigation of the propagation of a compact toroid along curved drift tubes,” *Nucl. Fus.*, vol. 44, pp. 982–986, 2004.
- [26] D. Liu, C. Xiao, A. Singh, and A. Hirose, “Bench test and preliminary results of vertical compact torus injection experiments on the STOR-M tokamak,” *Nucl. Fus.*, vol. 46, pp. 104–109, 2006.
- [27] P. Gierszewski, R. Raman, and D. Hwang, “Compact toroid fueling for ITER,” *Fus. Tech.*, vol. 28, pp. 619–624, 1995.
- [28] R. Raman and P. Gierszewski, “Compact toroid fuelling for ITER,” *Fus. Eng. Des.*, vol. 39–40, pp. 997–985, 1998.

References: Section 4

- [1] International Atomic Energy Agency, “ITER Technical Basis,” International Atomic Energy Agency, Tech. Rep., July 2001, no. 19 in the ITER EDA Documentation Series.
- [2] J. Degnan, R. J. Peterkin, G. Baca, J. Beason, D. Bell, M. Dearborn, D. Dietz, M. Douglas, S. Englert, T. Englert, K. Hackett, J. Holmes, T. Hussey, G. Kiuttu, F. Lehr, M. G.J., B. Mullins, D. Price, N. Roderick, E. Ruden, C. Sovinec, P. Turchi, G. Bird, S. Coffey, S. Seiler, Y. Chen, D. Gale, J. Graham, M. Scott, and W. Sommars, “Com-

- compact toroid formation, compression, and acceleration,” *Phys. Fluids B*, vol. 5, no. 8, pp. 2938–2958, 1993.
- [3] T. Murakami, T. Amano, K. Shimizu, and M. Shimada, “Transport analysis of tungsten impurity in ITER,” *J. Nucl. Mat.*, vol. 313–316, pp. 1161–1166, 2003.
- [4] R. Aymar, “The ITER Project,” *IEEE Trans. Plas. Sci.*, vol. 25, no. 6, pp. 1187–1195, 1997.
- [5] R. Raman and P. Gierszewski, “Compact toroid fuelling for ITER,” *Fus. Eng. Des.*, vol. 39–40, pp. 997–985, 1998.
- [6] M. Brown and P. Bellan, “Efficiency and scaling of current drive and refuelling by spheromak injection into a tokamak,” *Nucl. Fus.*, vol. 32, no. 7, pp. 1125–1137, 1992.

References: Section 5

- [1] International Atomic Energy Agency, “ITER Technical Basis,” International Atomic Energy Agency, Tech. Rep., July 2001, no. 19 in the ITER EDA Documentation Series.
- [2] J. Degnan, R. J. Peterkin, G. Baca, J. Beason, D. Bell, M. Dearborn, D. Dietz, M. Douglas, S. Englert, T. Englert, K. Hackett, J. Holmes, T. Hussey, G. Kiuttu, F. Lehr, M. G.J., B. Mullins, D. Price, N. Roderick, E. Ruden, C. Sovinec, P. Turchi, G. Bird, S. Coffey, S. Seiler, Y. Chen, D. Gale, J. Graham, M. Scott, and W. Sommars, “Compact toroid formation, compression, and acceleration,” *Phys. Fluids B*, vol. 5, no. 8, pp. 2938–2958, 1993.
- [3] L. Perkins, S. Ho, and J. Hammer, “Deep penetration fuelling of reactor-grade tokamak plasmas with accelerated compact toroids,” *Nucl. Fus.*, vol. 28, no. 8, pp. 1365–1378, 1988.

References: Section 6

- [1] S. Bozhokin, “Motion of a compact torus in a tokamak plasma,” *Sov. J. Plasma Phys.*, vol. 16, no. 10, pp. 702–705, 1990.
- [2] W. A. Newcomb, “Magnetohydrodynamic wave drag,” *Phys. Fluids B*, vol. 3, no. 8, pp. 1818–1829, 1991.
- [3] C. Xiao, A. Hirose, and W. Zawalski, “Trajectory of a compact toroid tangentially injected into a tokamak,” *Nucl. Fus.*, vol. 38, no. 2, pp. 249–256, 1998.
- [4] International Atomic Energy Agency, “ITER Technical Basis,” International Atomic Energy Agency, Tech. Rep., July 2001, no. 19 in the ITER EDA Documentation Series.
- [5] K. Baker, D. Hwang, R. Evans, R. Horton, H. McLean, S. Terry, S. Howard, and C. DiCaprio, “Compact toroid dynamics in the Compact Toroid Injection Experiment,” *Nucl. Fus.*, vol. 42, pp. 94–99, 2002.
- [6] P. Parks, “Refueling tokamaks by injection of compact toroids,” *Phys. Rev. Lett.*, vol. 61, no. 12, pp. 1364–1367, 1988.
- [7] Y. Suzuki, T. Hayashi, and Y. Kishimoto, “Theory and MHD simulation of fuelling by compact toroid injection,” *Nucl. Fus.*, vol. 41, no. 7, pp. 873–881, 2001.
- [8] L. Perkins, S. Ho, and J. Hammer, “Deep penetration fuelling of reactor-grade tokamak plasmas with accelerated compact toroids,” *Nucl. Fus.*, vol. 28, no. 8, pp. 1365–1378, 1988.
- [9] M. Nagata, A. Hatuzaki, M. Sugawara, and N. Fukumoto, “Compact torus injection into the HIST spherical torus plasmas,” in *Proceedings of the 33rd EPS Conference on Plasma Physics*, June 2006, pp. 4–7.
- [10] D. Biskamp, *Nonlinear Magnetohydrodynamics*, 1st ed., ser. Cambridge Monographs on Plasma Physics. Cambridge, UK: Cambridge University Press, 1993.

References: Section 7

- [1] D. Liu, C. Xiao, A. Singh, and A. Hirose, “Bench test and preliminary results of vertical compact torus injection experiments on the STOR-M tokamak,” *Nucl. Fus.*, vol. 46, pp. 104–109, 2006.
- [2] J. Degnan, R. J. Peterkin, G. Baca, J. Beason, D. Bell, M. Dearborn, D. Dietz, M. Douglas, S. Englert, T. Englert, K. Hackett, J. Holmes, T. Hussey, G. Kiuttu, F. Lehr, M. G.J., B. Mullins, D. Price, N. Roderick, E. Ruden, C. Sovinec, P. Turchi, G. Bird, S. Coffey, S. Seiler, Y. Chen, D. Gale, J. Graham, M. Scott, and W. Sommars, “Compact toroid formation, compression, and acceleration,” *Phys. Fluids B*, vol. 5, no. 8, pp. 2938–2958, 1993.
- [3] P. Gierszewski, R. Raman, and D. Hwang, “Compact toroid fueling for ITER,” *Fus. Tech.*, vol. 28, pp. 619–624, 1995.
- [4] R. Raman and P. Gierszewski, “Compact toroid fuelling for ITER,” *Fus. Eng. Des.*, vol. 39–40, pp. 997–985, 1998.

References: Section 8

- [1] M. Brown and P. Bellan, “Efficiency and scaling of current drive and refuelling by spheromak injection into a tokamak,” *Nucl. Fus.*, vol. 32, no. 7, pp. 1125–1137, 1992.
- [2] R. Raman, F. Martin, B. Quirion, M. St-Onge, J.-L. Lachambre, D. Michaud, B. Sawatzky, J. Thomas, A. Hirose, D. Hwang, N. Richard, C. Côté, G. Abel, D. Pinsonneault, J.-L. Gauvreau, B. Stansfield, R. Décoste, A. Côté, W. Zuzak, and C. Boucher, “Experimental Demonstration of Nondisruptive, Central Fueling of a Tokamak by Compact Toroid Injection,” *Phys. Rev. Lett.*, vol. 73, no. 23, pp. 3101–3104, 1994.

- [3] N. Fukumoto, Y. Inoo, M. Nomura, M. Nagata, T. Uyama, H. Ogawa, H. Kimura, U. Uehara, T. Shibata, Y. Kashiwa, S. Suzuki, S. Kasai, and JFT-2M Group, “An experimental investigation of the propagation of a compact toroid along curved drift tubes,” *Nucl. Fus.*, vol. 44, pp. 982–986, 2004.
- [4] D. Liu, C. Xiao, A. Singh, and A. Hirose, “Bench test and preliminary results of vertical compact torus injection experiments on the STOR-M tokamak,” *Nucl. Fus.*, vol. 46, pp. 104–109, 2006.
- [5] J. Degnan, R. J. Peterkin, G. Baca, J. Beason, D. Bell, M. Dearborn, D. Dietz, M. Douglas, S. Englert, T. Englert, K. Hackett, J. Holmes, T. Hussey, G. Kiuttu, F. Lehr, M. G.J., B. Mullins, D. Price, N. Roderick, E. Ruden, C. Sovinec, P. Turchi, G. Bird, S. Coffey, S. Seiler, Y. Chen, D. Gale, J. Graham, M. Scott, and W. Sommars, “Compact toroid formation, compression, and acceleration,” *Phys. Fluids B*, vol. 5, no. 8, pp. 2938–2958, 1993.
- [6] J. Davis, V. Barabash, A. Makhankov, L. Plöchl, and K. Slattery, “Assessment of tungsten for use in the ITER plasma facing components,” *J. Nucl. Mat.*, vol. 258–263, pp. 308–312, 1998.
- [7] I. Smid, M. Akiba, G. Vieider, and L. Plöchl, “Development of tungsten armor and bonding to copper for plasma-interactive components,” *J. Nucl. Mat.*, vol. 258–263, pp. 160–172, 1998.
- [8] J. Davis, K. Slattery, D. Driemeyer, and M. Ulrickson, “Use of tungsten coating on ITER plasma facing components,” *J. Nucl. Mat.*, vol. 233–237, pp. 604–608, 1996.
- [9] R. Raman, F. Martin, E. Haddad, M. St-Onge, G. Abel, C. Côté, N. Richard, N. Blanchard, H. Hai, B. Quirion, J.-L. LaChambre, J.-L. Gauvreau, G. Pacher, R. Décoste, P. Gierszewski, D. Hwang, A. Hirose, S. Savoie, B.-J. LeBlanc, H. McLean, C. Xiao, B. Stansfield, A. Côté, D. Michaud, and M. Chartré, “Experimental demonstration of tokamak fuelling by compact toroid injection,” *Nucl. Fus.*, vol. 37, no. 6, pp. 967–972, 1997.

- [10] T. Murakami, T. Amano, K. Shimizu, and M. Shimada, “Transport analysis of tungsten impurity in ITER,” *J. Nucl. Mat.*, vol. 313–316, pp. 1161–1166, 2003.
- [11] G. Bird, *Molecular Gas Dynamics and the Direct Simulation of Gas Flows*, 2nd ed., ser. Oxford Engineering Science Series. New York: Oxford University Press, 1994.
- [12] R. Raman and P. Gierszewski, “Compact toroid fuelling for ITER,” *Fus. Eng. Des.*, vol. 39–40, pp. 997–985, 1998.
- [13] International Atomic Energy Agency, “ITER Technical Basis,” International Atomic Energy Agency, Tech. Rep., July 2001, no. 19 in the ITER EDA Documentation Series.
- [14] M. Glugla, A. Busigin, L. Dörr, R. Haange, T. Hayashi, O. Kveton, R. Lässer, D. Murdoch, M. Nishi, R.-D. Penzhorn, and H. Yoshida, “The tritium fuel cycle of ITER-FEAT,” *Fus. Eng. Des.*, vol. 58–59, pp. 349–353, 2001.

References: Section 9

- [1] R. Raman and P. Gierszewski, “Compact toroid fuelling for ITER,” *Fus. Eng. Des.*, vol. 39–40, pp. 997–985, 1998.
- [2] International Atomic Energy Agency, “ITER Technical Basis,” International Atomic Energy Agency, Tech. Rep., July 2001, no. 19 in the ITER EDA Documentation Series.
- [3] P. Parks and F. Perkins, “A gyrotron-powered pellet accelerator for tokamak refuelling,” *Nucl. Fus.*, vol. 46, pp. 770–780, 2006.

References: Section 10

- [1] R. Raman, F. Martin, B. Quirion, M. St-Onge, J.-L. Lachambre, D. Michaud, B. Sawatzky, J. Thomas, A. Hirose, D. Hwang, N. Richard, C. Côté, G. Abel, D. Pinsonneault, J.-L. Gauvreau, B. Stansfield, R. Décoste, A. Côté, W. Zuzak, and C. Boucher,

- “Experimental Demonstration of Nondisruptive, Central Fueling of a Tokamak by Compact Toroid Injection,” *Phys. Rev. Lett.*, vol. 73, no. 23, pp. 3101–3104, 1994.
- [2] J. Degnan, R. J. Peterkin, G. Baca, J. Beason, D. Bell, M. Dearborn, D. Dietz, M. Douglas, S. Englert, T. Englert, K. Hackett, J. Holmes, T. Hussey, G. Kiuttu, F. Lehr, M. G.J., B. Mullins, D. Price, N. Roderick, E. Ruden, C. Sovinec, P. Turchi, G. Bird, S. Coffey, S. Seiler, Y. Chen, D. Gale, J. Graham, M. Scott, and W. Sommars, “Compact toroid formation, compression, and acceleration,” *Phys. Fluids B*, vol. 5, no. 8, pp. 2938–2958, 1993.
- [3] A. McLean, “The ITER Fusion Reactor And Its Role In The Development Of A Fusion Power Plant,” April 2002, presented at the 2nd International Youth Nuclear Congress, Daejeon, Korea, 2002.

A Glossary

A.1 Variables & Symbols, Roman

Table 4: Variables and symbols in paper, Roman

Symbol	Definition
a	Minor radius of tokamak [m]
B	Magnetic field of CT or tokamak, [T]
D	Deuterium, ${}^2_1\text{H}$
I	Newcomb drag parameter (see Section 6)
k	Dipole coupling strength, $0 < k < 1$
m_{CT}	CT mass [kg]
n	Neutron, ${}^1_0\text{n}$
r_{CT}	CT radius [m]
R	Radial coordinate
R_0	Major radius of tokamak [m]
T	Tritium, ${}^3_1\text{H}$
V_A	Alfvén velocity, $\frac{B_0}{\sqrt{\mu_0 n_0 m}}$
Z	Atomic weight, also vertical coordinate

A.2 Variables & Symbols, Greek

Table 5: Variables and symbols in paper, Greek

Symbol	Definition
α	Alpha particle, helium nucleus, ${}^4_2\text{He}$
β	Ratio of static pressure to magnetic pressure, $\beta = \frac{2\mu_0 p}{B^2}$
γ	Adiabatic ratio $\gamma = \frac{C_p}{C_v}$
θ	Sometimes signifies poloidal angle in polar coordinates (r, θ) in cross-section of torus
ρ	Plasma density (tokamak and CT)
τ	Normalization time for CT dynamics, $\tau = \frac{R_0}{V_A}$. Equal to the time it takes an Alfvén wave to cross the major radius of a tokamak.
ϕ	Toroidal angle in global tokamak cylindrical coordinates (R, ϕ, Z)

A.3 Terminology

Table 6: Terminology used in report

Term	Definition
Alfvén waves	MHD oscillations in a transverse direction to the dominant magnetic field. Along with acoustic (sound) waves, they carry energy away from an object such as a CT moving through a magnetized plasma.
CT	Compact toroid. Semi-stable plasma ring with embedded toroidal and poloidal magnetic fields and currents.
ITER	Large tokamak currently being built in Cadarache, France. Formerly stood for “International Thermonuclear Experimental Reactor”.
MARAUDER	CT acceleration project undertaken by United States Dept. of Defense in the early 1990s. Included both theoretical calculations and experimental verification.
MHD	Magnetohydrodynamics; the continuum theory linking the equations of fluid dynamics with Maxwell’s equations of electrodynamics. Usually considered in the “Ideal MHD” approximation of zero resistivity and low frequency.
Reconnection	Process by which magnetic field line topology, which in ideal MHD remains fixed, reorients itself to a lower-energy state. Releases stored magnetic energy as kinetic energy.
Tokamak	Currently most promising candidate arrangement for magnetic-confinement fusion reactor. Toroidally shaped reactor with poloidal and toroidal magnetic fields supported by large toroidal plasma current and external poloidal field magnets.

B Supporting Calculations

B.1 Fuelling Rate

CT fuelling rate = ITER (2001) pellet injection fuelling rate = $50 \text{ Pa m}^3 \text{ s}^{-1}$ @ NTP

$1 \text{ Pa m}^3 \text{ s}^{-1} = 9.9 \text{ cm}^3 \text{ s}^{-1} = 9.9 \times 10^{-6} \text{ m}^3 \text{ s}^{-1}$

NTP conditions (273.15 K, 101.325 kPa) $\rightarrow 44.62 \text{ mol m}^{-3}$

90%T/10%D effective molar mass = $2.916 \times 10^{-3} \text{ kg mol}^{-1}$

CT fuelling rate = $4.95 \times 10^{-4} \text{ m}^3 \text{ s}^{-1} = 0.022087 \text{ mol s}^{-1} = 6.44 \times 10^{-5} \text{ kg s}^{-1}$

Firing rate of 50 Hz, one CT injector, CT mass = 1.29 mg

B.2 Euler-Lagrange Equations for CT Motion

Set of coordinates $(R, \phi, Z, \alpha, \beta, \gamma)$. Convert variables to nondimensional form as follows (following Bozhokin (1990)):

$$\dot{Q} \equiv \frac{dQ}{d\tau} \qquad \tau \equiv \frac{t}{t_0} = \frac{V_A}{R_0} t \qquad (7)$$

$$Y_1(\tau) \equiv \frac{R}{R_0} \qquad V_1(\tau) \equiv \dot{Y}_1 = \frac{1}{V_A} \frac{dR}{dt} \qquad (8)$$

$$Y_2(\tau) \equiv \phi \qquad V_2(\tau) \equiv \dot{Y}_2 = t_0 \frac{d\phi}{dt} \qquad (9)$$

$$Y_3(\tau) \equiv \frac{Z}{a} \qquad V_3(\tau) \equiv \dot{Y}_3 = \frac{t_0}{a} \frac{dz}{dt} \qquad (10)$$

$$Y_4(\tau) \equiv \alpha \qquad V_4(\tau) \equiv \dot{Y}_4 = t_0 \frac{d\alpha}{dt} \qquad (11)$$

$$Y_5(\tau) \equiv \beta \qquad V_5(\tau) \equiv \dot{Y}_5 = t_0 \frac{d\beta}{dt} \qquad (12)$$

$$Y_6(\tau) \equiv \gamma \qquad V_6(\tau) \equiv \dot{Y}_6 = t_0 \frac{d\gamma}{dt} \qquad (13)$$

$$(14)$$

Then Euler-Lagrange equations for V become:

$$\dot{V}_1 = Y_1 V_2^2 + \frac{E_0}{Y_1^3} + \frac{C_0}{Y_1^2} A_0 - Q_0 V_1 \quad (15)$$

$$\dot{V}_2 = \frac{-2V_1 V_2}{Y_1} - \frac{C_0}{Y_1^3} \frac{dA_0}{d\phi} - Q_0 V_2 \quad (16)$$

$$\dot{V}_3 = -Q_0 V_3 \quad (17)$$

$$\dot{V}_4 = -\frac{D_0}{Y_1} \frac{dA_0}{dY_4} \quad (18)$$

$$\dot{V}_5 = -\frac{D_0}{Y_1} \frac{dA_0}{dY_5} \quad (19)$$

$$\dot{V}_6 = -\frac{D_0}{Y_1} \frac{dA_0}{dY_6} \quad (20)$$

Where the nondimensional constants (A_0, C_0, D_0, E_0, Q_0) are the same as for Bozhokin (1990) and Xiao (1998a) except for A_0 :

$$A_0 = \cos Y_4 \sin Y_5 \cos Y_6 \sin Y_2 + \sin Y_4 \sin Y_6 \sin Y_2 \\ + \sin Y_4 \cos Y_6 \cos Y_2 - \cos Y_4 \sin Y_5 \sin Y_6 \cos Y_2 \quad (21)$$

$$C_0 = k \frac{\rho_0}{\rho_{CT}} \frac{B_{CT}}{B_0} \quad (22)$$

$$D_0 = \frac{5}{2} k \frac{\rho_0}{\rho_{CT}} \frac{B_{CT}}{B_0} \frac{R_0^2}{r_{CT}^2} \quad (23)$$

$$E_0 = \frac{\rho_0}{\rho_{CT}} \quad (24)$$

$$Q_0 = I \frac{3}{2} \frac{R_0}{r_{CT}} \frac{\rho_0}{\rho_{CT}} \quad (25)$$

C Design Drawings

Please see Figures 11, 12, and 13.

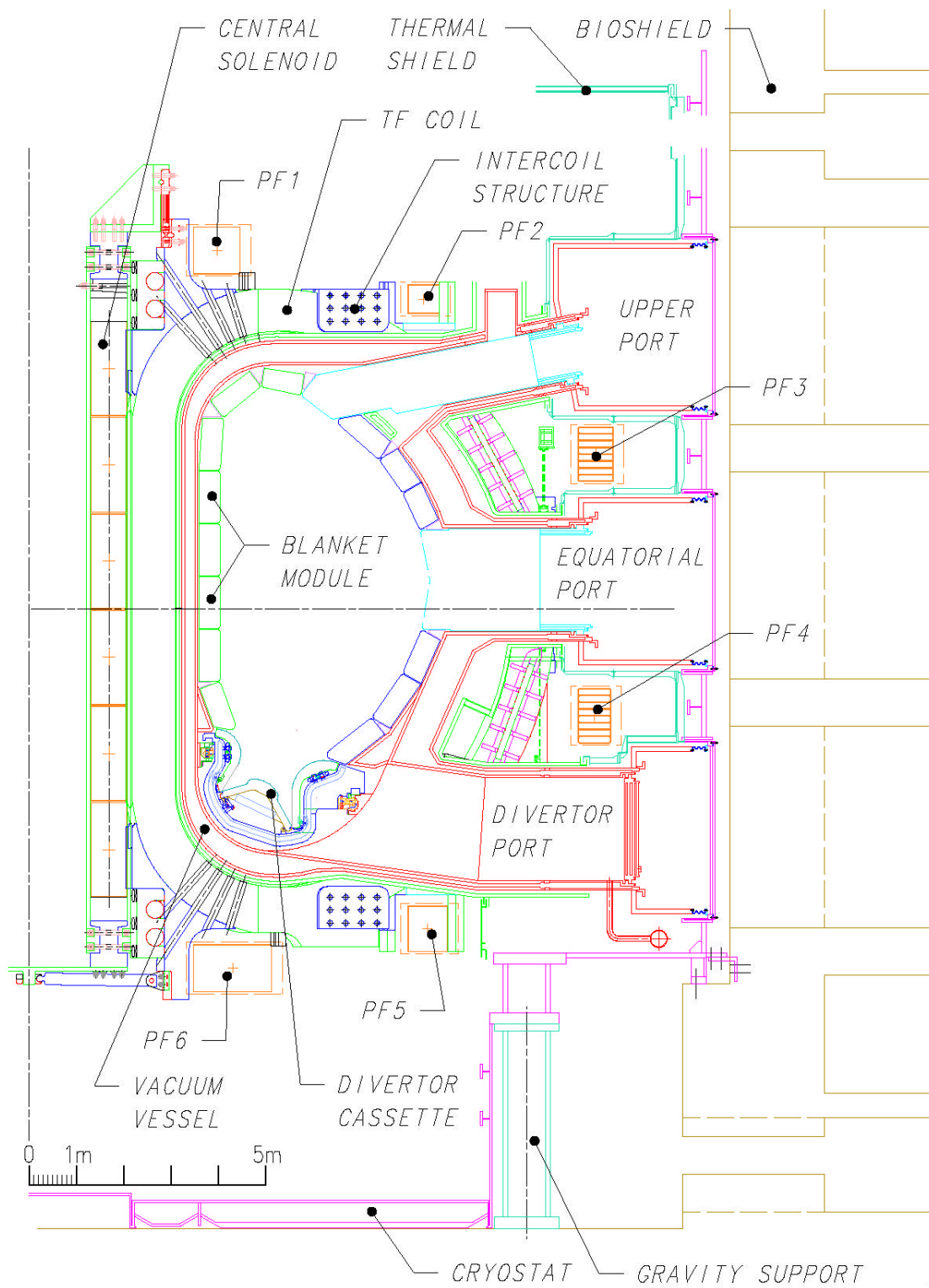


Figure 11: Scaled drawing of ITER tokamak and injection ports. Distance is 9.96 m from inner wall of bioshield to reactor first wall at a downward angle of 12° . Courtesy International Atomic Energy Agency, Vienna, 2001.

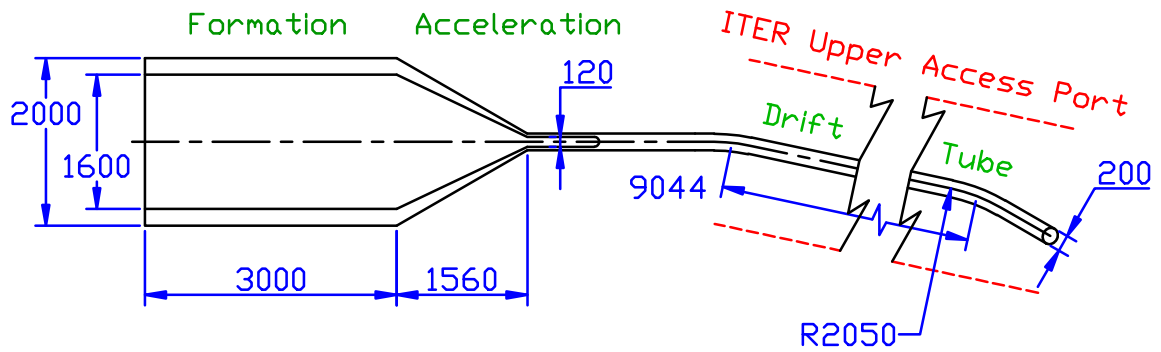


Figure 12: Details of CT injector orientation showing formation and acceleration regions, as well as drift tube and emission region.

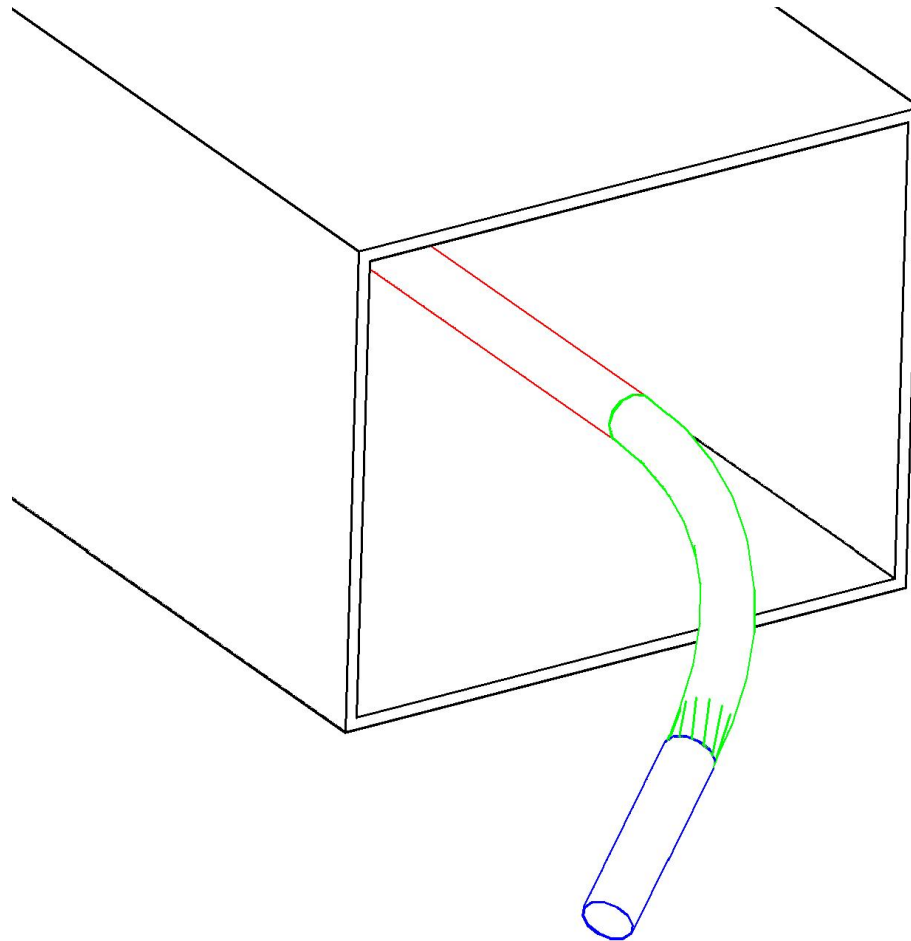


Figure 13: 3D render of end of barrel showing straight 10 m section of drift tube (red), curved region (green), and straight end (blue). Large rectangular duct is the upper port (2 m × 2.5 m).